

EVALUATION OF URBANIZATION INFLUENCES ON URBAN CLIMATE WITH REMOTE SENSING AND CLIMATE OBSERVATIONS

George Xian¹ and Mike Crane²

¹SAIC/²USGS National Center for Earth Resources Observation and Science, Sioux falls, SD 57198

xian@usgs.gov

KEY WORDS: Urban, Impervious surface, climate, remote sensing

ABSTRACT:

Remote sensing data were utilized to assess urban land cover and its thermal characteristics through mapping sub-pixel impervious surfaces and assessing thermal infrared images. Landsat imagery was used to calculate variation in urban imperviousness from 1995 to 2002 in the Tampa Bay watershed, Florida. The urban-rural boundary and urban development density were defined by selecting certain imperviousness threshold values. Landsat thermal bands were processed to obtain radiant surface temperatures (T_b) to investigate the urban heat island (UHI) effect associated with increasing impervious surfaces both spatially and temporally. Analysis shows significant differences in T_b values associated with different percentages of imperviousness. Surface heat characteristics exhibit a close relationship with impervious surface intensities. An inverse relationship between imperviousness and Normalized Difference Vegetation Index (NDVI) was determined for several urban areas. Impacts of urbanization on the climate conditions of urban and suburban areas in the Tampa Bay watershed have been investigated by analyzing the change of T_b , imperviousness, NDVI using data collected from Landsat and historical climate information in the region. Local climate change was studied using multi-decade temperature and other climate observation information. Our results suggest that increasing urban imperviousness has a certain effect on the monthly average minimum surface temperature and seasonally averaged temperature changes in the watershed area. The information on the spatial and temporal distribution of imperviousness that objectively identifies and quantified urban land use intensity and change patterns also outlines UHI effect in the watershed.

1. INTRODUCTION

Urban growth, both in population and in areal extent, transforms the landscape from natural cover types to increasingly impervious urban land. The result of this change can have significant effects on local weather and climate (Landsberg, 1981). One of the most familiar is the urban heat island (UHI) phenomenon that represents temperatures in urban area are a few degrees higher than in surrounding non-urbanized areas.

Considerable research has performed in using remotely sensed information to detect thermal

characteristics of urban surfaces. Carlson *et al.* (1977) pointed out that warmer than surrounding thermal features were associated with urban land use and could be identified from infrared radiative surface temperature. Matson *et al.* (1978) used NOAA 5 satellite nighttime thermal infrared imagery to obtain maximum urban-rural temperature differences ranging from 2.6 to 6.5⁰C for more than 50 selected cities in the midwestern and northeastern United States. Price (1979) showed that for many large cities satellite sensed temperatures were 10-15⁰C warmer than surrounding rural areas in the New York City – New England region. To estimate UHI effects at local or regional scales, finer resolution

remote sensing data is essential (Quattrochi *et al.*, 2000; Streutker, 2002). In general, residential land cover was relatively cool ($\sim 20^{\circ}\text{C}$), whereas, the central business district (CBD) was warm to hot at approximately 35°C (Quattrochi *et al.*, 2000). It has been shown that land cover change associated with urban growth can alter surface temperature significantly (Weng, 2001).

Roth *et al.* (1989) compared daytime and nighttime urban thermal patterns by using urban heat island data derived from satellite remote sensing. Their results suggested that satellite-derived UHI intensity was strong in daytime. Urbanization generally modifies land surface and atmospheric boundary conditions and leads to a modified thermal climate that is warmer than the surrounding non-urbanized areas, particularly at night (Voogt and Oke, 2003). Karl *et al.* (1988) estimated urbanization effects on the United States climate record by using climate records and population data to delineate urban and rural areas. Their results indicated that annual mean temperatures at stations populated areas of 10,000 people or more were 0.1°C warmer than nearby stations located in rural areas with population less than 2,000. Urbanization had significant impact on temperature diurnal minima, means and range. Urbanization and its attendant impacts on local and regional climate counted for half of the decrease in diurnal temperature range in the U.S. (Kalnay and Cai, 2003). Kalnay and Cai also cited other studies that found the impact depended on whether population data or satellite imagery were used to classify urban and rural areas.

Voogt and Oke (2003) summarized different approaches for using thermal remote sensing information in urban climate studies and recommended use of more fundamental surface descriptors beyond qualitatively based land use data to describe the urban surface in the thermal remote sensing of urban areas. Others have used urban-rural differences in the vegetation index (NDVI) as a measure of the surface properties to

estimate urban and rural minima air temperature (Gallo and Owen, 1999; Gallo and Owen, 2002; Gallo *et al.*, 2002; Weng *et al.*, 2004). Wilson *et al.* (2003) also suggested that mean T_b and NDVI values were significantly different for various zoning categories.

This study uses Landsat Thematic Mapper (TM) and Enhanced Thematic Mapper plus (ETM+) data to analyze the influence of urbanization on surface radiant temperature in Tampa bay, Florida. Urban extent and development intensity are determined from measurements of percent impervious surface area (ISA) obtained from Landsat remote sensing data. Both the spatial and temporal distributions of T_b associated with ISA are evaluated. Historical climate information collected by the Southeast Regional Climate Center, South Carolina, USA are utilized to study 50-year temperature trends in the watershed and to assess the effect of urbanization on the local climate.

2. BACKGROUND

2.1 Study Area

Tampa Bay estuary, located on the Gulf coast of west-central Florida, covers an areal extent of approximately $1,030\text{ km}^2$. The watershed containing Tampa Bay encompasses approximately $6,600\text{ km}^2$ (Fig. 1). Urban land use extent in the Tampa Bay area has increased approximately 7 times the last century (Xian and Crane, 2003). To monitor changes in urban land use/cover in a timely and cost-effective manner, the physical parameter, “anthropogenic impervious surface”, defined as impenetrable surfaces such as rooftops, roads, and parking lots, was used as an indicator of the spatial extent and intensity of development. This parameter was chosen because the amount and change of ISA is clearly linked to major urban land cover types and their changes.

2.2 The Measurement of Urban ISA

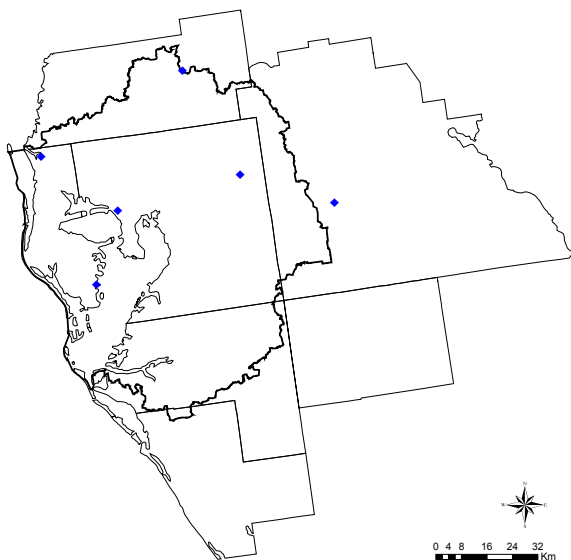


Fig 1. The Tampa watershed and associated counties. The blue dots indicate weather station locations.

Urban areas are heterogeneous and most Landsat pixels consist of a mixture of different surfaces. To accurately estimate urban land use/cover, the Sub-pixel Imperviousness Change Detection (SICD) method was used with remote sensing data to spatially quantify urban land cover/land use change (Yang *et al.*, 2003; Xian, *et al.*, in press). This method uses high-resolution digital imagery to develop training data for representing urban land cover heterogeneity, and medium-resolution Landsat imagery to extrapolate ISA over large regions. This technique has been implemented by the U.S. Geological Survey's (USGS) Geographic Analysis and Monitoring (GAM) program for the production of an imperviousness layer as a component of the National Map.

The process of mapping ISA and related land-cover change data sets using SICD involves the following steps: (1) development of training data using high-resolution digital orthophoto quarter quadrangles (DOQQs), (2) selection of predictive variables and initial regression tree modeling, (3) final spatial modeling and mapping with Landsat

TM/ETM+, and (4) ISA change detection and interpretation.

The current study used DOQQs produced by the USGS during the late 1990s to derive training data for a regression tree model and test for imperviousness mapping. The DOQQs were scanned from color infrared photographs acquired from the National Aerial Photography Program. Each DOQQ consisted of three spectral bands — green, red, and near infrared — with a nominal spatial resolution of 1 m. Training pixels classified as urban in 1-meter grids from the DOQQ were used to calculate percent ISA for each Landsat pixel. The result was a 30-meter resolution raster ISA image.

3. METHODS

3.1 Image Pre-processing

Landsat TM and ETM+ images from 1994-1995, 2000-2001 and 2002 were used in this study. All images were preprocessed by the U.S. Geological Survey (USGS) National Center for Earth Resources Observation and Science (EROS) to correct radiometric and geometrical distortions of the images to level 1G products. Possible geolocation errors due to terrain effect were corrected using the 1-arc second National Elevation Dataset (NED). All images were rectified to a common Universal Transverse Mercator coordinate system. Bands 1 through 5 and 7 were utilized at a spatial resolution of 30 m. After being processed using the standard geometric and radiometric correction methods, the thermal bands had their original pixel sizes of 120 m for TM and 60 m for ETM+ images were resampled to 30 m using the nearest neighbor algorithm to match the pixel size of other spectral bands.

3.2 Determination of T_b , NDVI from TM and ETM+

The above corrections then resulted in digital number (DN) images that are measures of at-satellite radiance. DNs in each band were

converted first to at-satellite radiance and then to at-satellite reflectance using the following equations:

$$L_{\lambda} = \text{Gain}_{\lambda} \cdot \text{DN}_{\lambda} + \text{Bias}_{\lambda} \quad (1)$$

$$\rho_{\lambda} = (\pi L_{\lambda} d^2) / (\text{ESUN}_{\lambda} \cdot \sin(\theta)) \quad (2)$$

where L_{λ} is at sensor radiance, Gain_{λ} = slope of radiance/DN conversion function, Bias_{λ} = intercept of the radiance/DN conversion function. Gain and Bias values are provided in metadata accompanying each TM/ETM+ image (Landsat Project Science Office, 2002). ρ_{λ} is unitless at-satellite reflectance for the TM/ETM+ bands (1-5, 7), θ = solar zenith angle and ESUN_{λ} = mean solar exoatmospheric irradiance.

Radiance values from TM band 6 and ETM+ band 9 were transformed to radiant surface temperature values using the following equation

$$T_b = K2 / \ln(K1 / L_{\lambda} + 1) \quad (3)$$

where $K2$ = calibration constant 2 (1260.56 for TM and 1282.71 for ETM+), $K1$ = calibration constant 1 (607.76 for TM and 666.09 for ETM+), and L_{λ} is defined in (1). The unit of T_b is Kelvin degree.

Reflectance values from the visible (ρ_1) and near-infrared (ρ_2) bands of ETM+ images were used to compute NDVI values using the formula $\text{NDVI} = (\rho_2 - \rho_1) / (\rho_2 + \rho_1)$. The final results were then normalized to a scale of 1-100.

All T_b and NDVI were calculated from scenes in path 17 since scenes in path 16 were acquired in different dates and had significant differences.

4. RESULTS

4.1 Significance of Differences in Imperviousness and T_b

Inspection of the imperviousness maps showed that the 10% threshold captured almost all development including low, medium, and high-density residential areas, as well as the central business district (CBD). This agreed with the analysis made by Jantz *et al.* (2003) for the Baltimore-Washington metropolitan area where

the 10% threshold was selected to represent the urban area. The Tampa Bay watershed ISA results indicated that the area with percent

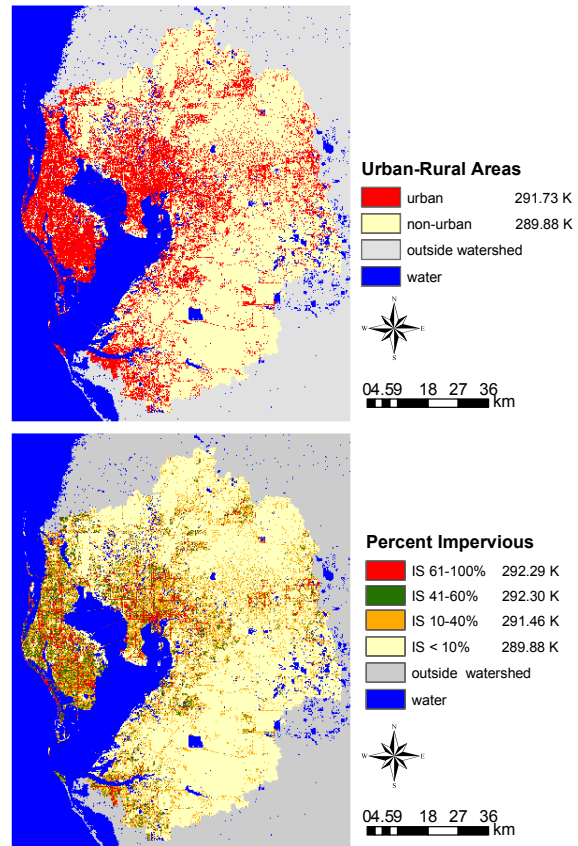


Fig. 2. Urban and T_b in 2002. Upper is the urban and rural areas defined by 10% ISA threshold. Different ISA intensities and associated T_b are shown on lower.

imperviousness greater than 10% was 995 km² in 1994, 1359 km² in 2000, and 1721 km² in 2002. Pixels were classified as urban when the ISA as equal to or greater than 10%, and those pixels of less than 10% were classified as non-urban. In order to isolate the UHI in each image, water was masked prior to T_b estimation. After the water pixels were removed, temperatures of remaining pixels were re-mapped according to each ISA group. Temperature histograms were created for each T_b map. Some extremely high and low temperatures associated with ISA were had been retained, e.g., low temperature caused by shadows in high-density urban area, and high

temperatures caused by image noise. The final radiant surface temperature map was produced by removing any pixels with a temperature less or greater than two standard deviations (2σ) minus or plus the mean. The mean T_b for each imperviousness category and differences between T_b in urban and T_b in rural area for three dates are presented in Table 1. Significant difference between T_b in $ISA \geq 10\%$, urban area, and T_b in $ISA < 10\%$, rural area can be found in three dates results. The 2.26°C difference in 2000 marks a strong UHI effect in the watershed. Another significant effect is the increase in the magnitudes of different urban development densities subtraction from the rural. In 2000 the difference of mean T_b in high-density urban area to the T_b in rural area reaches to 3.16°C . Combining ISA and associated mean T_b together, the magnitude and spatial extent of the heat island in 2002 is shown in Fig. 2. The spatial extent of UHI suggests that urban development raised T_b by replacing natural land with impervious land such as concrete, stone, and metal.

	ISA < 10%	ISA 10 - 40%	ISA 41- 60%	ISA >60%	ISA \geq 10%
1994	290.76	291.16	291.21	291.24	291.19
ΔT	0	0.40	0.45	0.48	0.44
2000	301.12	303.08	303.74	304.28	303.38
ΔT	0	1.96	2.62	3.16	2.26
2002	289.88	291.46	292.30	292.29	291.77
ΔT	0	1.58	2.42	2.41	1.89

Table 1. Mean T_b in different ISA and its difference from T_b in $ISA < 10\%$.

4.2 Imperviousness, NDVI and T_b

To get a general understanding of NDVI associated with different ISAs, we randomly selected 71 points in the watershed to create a statistical summary. Fig.3 depicts NDVI values associated with different percent ISA. The linear regression of these points yields a coefficient of determination value $r^2 = 0.667$ and indicates an inverse linear relationship between T_b and NDVI

in that watershed. The lower imperviousness has higher NDVI value because of the predominance of vegetation cover. In contrast, the higher ISA coverage associated with high-density urban areas such as high-density residential, commercial and industrial land possessed lower NDVI values. A similar inverse relationship (not shown) between T_b and NDVI was found from these selected data, however, r^2 value was only 0.188. This suggests a negative, moderately low correlation between T_b and NDVI in the watershed.

4.3 Climate Data Analysis

The humid sub-tropical climate of the area is, characterized by warm, wet summers and mild winters. Urban development is replacing the natural environment with nearly non-evaporating, non-transpiring ISA and modifying the local climate. Temperature obtained from Landsat thermal infrared band is the brightness temperature (also known as blackbody temperature). It differs from land surface temperature that can be obtained through emissivity correction, or air temperature that is controlled by both atmospheric conditions and radiation from the sun and the earth surface. We utilized historical climate data collected by the Southeast Regional Climate Center, South Carolina, USA to investigate multi-decade climate change in the watershed area. Records including monthly and annually averaged temperature and precipitation have been analyzed for the region. Six stations shown in Fig. 1 are situated at Tampa, St. Petersburg, St Leo, Plant City, Bartow, and Tarpon Springs, and are marked by blue dots provided annual monthly average minimum temperature from 1948 to 2003. The minimum temperature has an increasing trend after the middle 1970s. The linear regression line with least-square $r^2 = 0.389$ shows an annual increase rate of 0.02°C . It is known that the near-surface air temperature UHI effect mostly takes place at night, when radiative cooling differences between urban and rural areas reach

the strongest strengths. The warmer air temperature

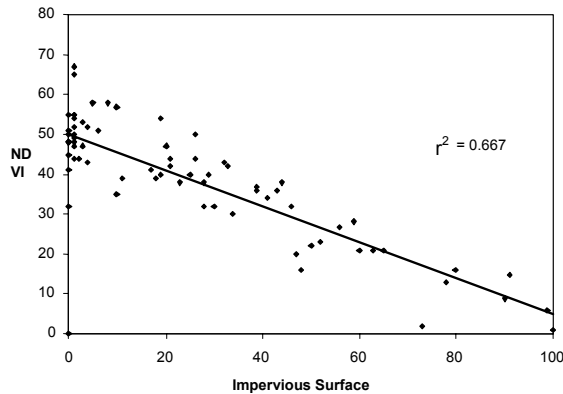


Fig. 3. Linear regression of NDVI and imperviousness for randomly selected locations.

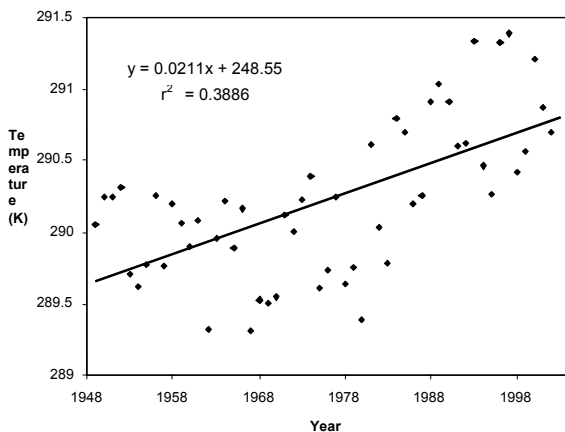


Fig. 4. Average of monthly minimum temperature for six stations.

of the night in the urban area raises daily low temperature (usually is the minimum temperature of the day). This increase in the long-term minimum temperature over the Tampa Bay is believed to be directly related to the UHI effect.

5. CONCLUSIONS

Urban development intensity and spatial extent can be characterized by using satellite remote sensing data through mapping the impervious surface distributions. This research has shown that different urban development intensities — defined

by different percent imperviousness — have significant effects on radiant surface temperature within the Tampa Bay watershed. Higher mean T_b values are associated with higher percent imperviousness. In addition, an inverse relationship between NDVI and ISA characterized the area. An UHI effect exists in the Tampa Bay region and it has been identified by combining T_b and ISA with 10% threshold. Averaged multi-decade climate data in the watershed indicates that the annual monthly minimum temperature has a 0.2°C per-decade increasing trend in the area. The long-term impact of UHI effect may modify climate condition in the region.

ACKNOWLEDGEMENTS

This research was performed under U.S. Geological Survey contract 03CRCN0001. We wish to thank Mr. Cory McMahon for preprocessing Landsat data and producing part of the impervious surface data.

REFERENCES

- Carlson, T.N., Augustine, J.A., and Boland, F.E. 1977. Potential application of satellite temperature measurements in the analysis of land use over urban areas. *Bulletin of the American Meteorological Society*, 58(12), pp. 1301-1303.
- Gallo, K.P. and Owen, T.W., 1999. Satellite-Based adjustments for the urban island temperature bias. *J. Applied. Meteorology.*, 38, pp. 806-813.
- Gallo, K.P. and Owen, T.W., 2002. A sampling strategy for satellite sensor-based assessments of the urban heat-island bias. *Int. J. Remote Sensing*, 23(17), pp. 1935-1939.
- Gallo, K., Adegoke, J.O., Owen, T.W., and Elvidge, C.D., 2002. Satellite-based detection

- of global urban heat-island temperature influence. *J. Geophys. Res.*, 107(24), ACL 16.
- Jantz, C.A., Goetz, S.J. & Shelley, M.K., 2003. Using the SLEUTH urban growth model to simulate the impacts of future policy scenarios on urban land use in the Baltimore-Washington metropolitan area. *Environment and Planning B: Planning and Design*, 30, pp. 251-271.
- Kalnay, E. & Cai, M., 2003. Impact of urbanization and land-use change on climate. *Nature*, 423(29), pp. 528-531.
- Karl, T., Diaz, H.F., Kukla, G., 1988. Urbanization: Its detection and effect in the United States climate record. *J.Climate*, 1, pp. 1099-1123.
- Landsberg, H.E., 1981. *The Urban Climate*. New York: Academic Press.
- Landsat Project Science Office (2002). Landsat 7 Science Data User's Handbook. URL: http://ltpwww.gsfc.nasa.gov/IAS/handbook/handbook_toc.html (accessed 10 Dec. 2004).
- Matson, M., McClain, E.P., McGinnis, D.F. & Pritchard, J.A., 1978. Satellite Detection of urban heat islands. *Mon. Wea. Rev.*, 106, pp. 1725-1734.
- Price, J., 1979. Assessment of the urban heat island effect through the use of a satellite data. *Mon. Wea. Rev.*, 107, pp. 1554-1557.
- Quattrochi, D. A., Luvall, J.C., Richkman, D.L., Estes, M.G., Laymon, C.A. & Howell, B.F., 2000. A decision support information system for urban landscape management using thermal infrared data. *Photogrammetric Engineering & Remote Sensing*, 66(10), pp. 1195-1207.
- Roth, M., Oke, T.R. & Emery, W.J., 1989. Satellite-derived urban heat island from three coastal cities and the utilization of such data in urban climatology. *Int. J. Remote Sensing*, 10(11), pp. 1699-1720.
- Streutker, D.R., 2002. A remote sensing study of the urban heat island of Houston, Texas. *Int. J. Remote Sensing*, 23(13), pp. 2595 – 2608.
- Voogt, J.A. & Oke, T.R., 2003. Thermal remote sensing of urban climates. *Remote Sensing of Environment*, 86, pp. 370-384.
- Weng, Q., 2001. A remote sensing-GIS evaluation of urban expansion and its impact on surface temperature in the Zhujiang Delta, China. *Int. Remote Sensing*, 22(10), pp. 1999-2014.
- Weng, Q., Lu, D. & Schubring, J., 2004. Estimation of land surface temperature-vegetation abundance relationship for urban heat island studies. *Remote Sensing of Environment*, 89, pp. 467-483.
- Wilson, J.S., Clay, M., Martin, E., Struckey, D. & Vedder-Risch, K., 2003. Evaluating environmental influences of zoning in urban ecosystems with remote sensing. *Remote Sensing Environment*, 86, pp. 303-321.
- Xian, G. and Crane, M., 2003. Impacts of urban development on seagrass in Tampa Bay. *Proceedings of the 19th National Environmental Monitoring Conference*, Arlington, Virginia, U.S.A., No.23.
- Xian, G., Yang, L., Klaver, J. M., Hossain, N. (in press). Measuring urban sprawl and extent through multi-temporal imperviousness mapping. USGS Urban Dynamic Topic Report, USGS Circular.
- Yang, L., Xian, G., Klaver, J.M. & Deal, B., 2003. Urban land-cover change detection through sub-pixel imperviousness mapping using remotely sensed data. *Photogrammetric Engineering & Remote Sensing*, 69(9), 1003-1010.